A Linear Prediction Land Mine Detection Algorithm for Hand Held Ground Penetrating Radar

K. C. Ho, *Senior Member, IEEE*, and Paul D. Gader, *Senior Member, IEEE*

***Abstract*—Land mine detection using ground penetrating radar (GPR) is a difficult task because the background clutter characteristics are nonstationary and the land mine signatures are inconsistent. A particularly difficult scenario is the case for which a GPR is mounted on a hand held device with no position or velocity information available to a signal processing algorithm. This paper proposes the use of linear prediction in the frequency domain for land mine detection in this scenario. A frequency domain clutter vector sample is partitioned into subbands. Each subband is modeled by a linear prediction model; the current vector sample is expressed as a linear combination of the past few vector samples plus random noise. The detector first computes the Maximum Likelihood estimate of the prediction coefficients, and then uses the generalized likelihood method to determine if a land mine is present. The effect of subband processing on the accuracy of the detector is evaluated. Detection results are presented on data collected from a variety of geographical locations. The data sets contain over 2300 mine encounters of different size, shape and content, and a larger number of measurements from locations with no mines. The proposed detector is compared to the baseline differential energy detector. The proposed algorithm reduces the false alarm rate by 60% for all the targets at 90% probability of detection, and 70% for the deep anti-tank mines at 90% probability of detection.**

***Index Terms*—Detection, frequency domain, ground penetrating radar, land mine, linear prediction, maximum likelihood, subband processing.**

I. Introduction

ACCORDING to an estimate from the United Nations, between 60 to 100 million mines lie buried around the world, claiming 10 000 deaths annually and at least twice as many seriously injured. Many victims are small children and elderly villagers in poor nations. Finding buried land mines is an important and difficult problem. Metal detectors are the almost universally available fielded devices for land mine detection. Metal detectors have great difficulty detecting land mines that are made of plastic or have low metal content. Ground Penetrating Radar (GPR) is an emerging technique for land mine detection [1]–[4] that can detect plastic or low metal content land mines. This paper focuses on land mine detection using GPR.

Prototype GPR systems are usually vehicle mounted or hand held. Vehicle mounted systems have a GPR attached to the front of a vehicle and capture the radar signals at equally spaced positions as the vehicle moves. The vehicle speed and the height of GPR above the ground surface are relatively constant. Land mines in this case often produce stable signatures, such as hyperbolic shapes, for detection. In addition, a vehicle mounted system allows a look ahead of several samples before making a detection decision, since there is a finite distance between the vehicle front and its wheels.

Gader *et al.* [5], [6] recently proposed and field tested a gradient based method that can effectively identify the roughly hyperbolic shapes produced by land mines for detection. Fuzzy logic fusion is also applied to further improve detection accuracy. Techniques based on Hidden Markov Models are currently under investigation [7]–[10].

A second type of mine detection system uses the GPR in a hand held unit. An operator carries the unit and sweeps it across the ground. Because of the human factor, the sweeping speed and the sensor-to-ground distance are varying. Hence the GPR land mine signatures are inconsistent and the hyperbolic signatures as observed in the vehicle based system are not present except for very big mines. The position and velocity of the sensor are not measured and are not available to any detection algorithm. All these factors make land mine detection using a hand held GPR is a difficult task. Furthermore, the detection needs to be causal and no future look ahead is allowed. The purpose of this work is to develop an effective algorithm that does not rely heavily on the mine signatures, and is relatively insensitive to the variations in the sweeping speed and radar height to ground distance.

Generally speaking, two kinds of commonly used GPR for land mine detection are pulse radar and frequency stepped continuous wave (FSCW) radar. Pulse radar sends out short duration pulses and samples the returned signals to obtain the radar response. On the other hand, FSCW sends out stepped radio frequency (RF) signal to the ground and measures the return. The current hand held GPR for detection algorithm development is a FSCW radar with equal frequency increments [11], [12]. The bandwidth of the radar hardware is in the order of gigahertz (GHz). The sampling rate is about 80 Hz.

The difficulty of the hand held land mine detection problem can be illustrated by observing the data. Fig. 1 shows the magnitude plot of FSCW GPR data in the frequency domain, where the y-axis corresponds to frequency index and the x-axis corresponds to the position index. The upper sub-window indicates the positions where land mines occur. The data were collected by sweeping the GPR back and forth over the same land mine four times. Although the data were collected over the same land mine, the signatures in the four land mine sections are different.

Manuscript received May 19, 2001; revised March 7, 2002. This work was supported in part by the U.S. Army Countermine Division under Grants DAAB15-99-C-1010 and DAAB15-00-D-1009, and by the OSD funded Multidisciplinary Research on Mine Detection and Neutralization Systems under Grant DAAG55-97-1-0014.

K. C. Ho is with the University of Missouri, Columbia, MO 65211 USA (e-mail: hod@missouri.edu).

P. D. Gader is with the University of Florida, Gainesville, FL 32611 USA (e-mail: pgader@cise.ufl.edu).

Publisher Item Identifier 10.1109/TGRS.2002.800276.

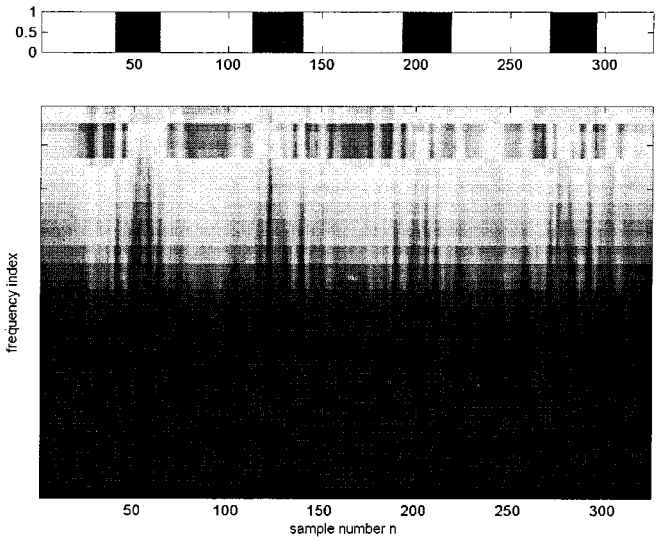

Fig. 1. Magnitude plot of GPR data collected over a landmine. The sensor is moved back and forth over the landmine four times.

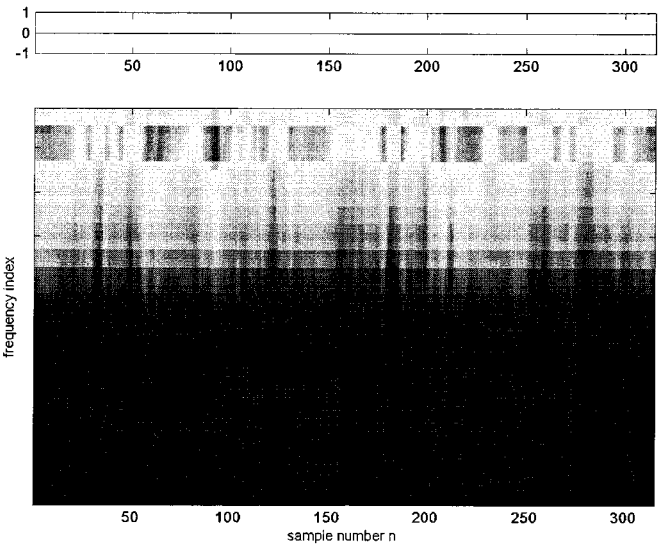

Fig. 2. Magnitude plot of GPR data in clutter. The data is collected over clutter in the same way as it is collected over a mine.

Fig. 2 is the magnitude plot of GPR data collected from clutter. Clutter here refers to any region of ground that does not contain a buried land mine. The clutter data are very similar to those from the land mine. Land mine detection using GPR in a hand held unit is a challenging task. The difficulty is due to the inconsistency of landmine signatures and the nonstationary behavior of background clutter.

A previous work by Brunzell [13] subtracted the background signal from a hand held GPR return and applied an energy detector to detect shallow objects under the ground. It considered the detection of four different kinds of objects under laboratory conditions that had relatively stable background clutter characteristics. The clutter characteristics in the present system are time-varying and background subtraction does not provide satisfactory results.

This paper proposes the use of a linear prediction (LP) technique for land mine detection in a hand held system. The proposed method models the GPR clutter data using a linear prediction model, and applies the constant false alarm rate (CFAR) technique [14]–[16] on the clutter likelihood function for detection. The linear prediction coefficients are made adaptive to account for the time-varying behavior of background clutter. At each new sample location, the prediction coefficients are estimated through the Maximum Likelihood (ML) method. The estimated coefficients are then used to form the test statistic for detection. To further capture the random nature of background clutter, the detection threshold is adaptive.

Most GPR land mine detection techniques apply processing in the range domain. This paper proposes processing in the frequency domain. An advantage of frequency domain processing is that the GPR data can be split into several subbands for processing. Subband processing can take into account the distinct reflection characteristics of land mines at different frequency bands and thereby increases the detection accuracy.

The use of LP for clutter reduction was previously proposed by Farina *et al*. [17]. This method assumes stationary clutter and the computation of LP coefficients is done over the clutter area. The proposed algorithm here deals with nonstationary clutter environment and the LP coefficients are computed adaptively at several subbands. A technique that uses subband processing to enhance signal is found in [18]. This subband processing method, however, does not use LP and requires two separate channel measurements where one contains the incident and the other the backscattered signal.

Some techniques that are based on ML principle for land mine detection are available in literature. Brunzell [19] applied generalized Likelihood ratio test to detect land mines. The technique assumes constant ground reflection and mine signals, and it is not be applicable to our case that encounters highly nonstationary background clutter characteristics. In addition, it does not use linear prediction model. Uschkeret [20] also applied similar Likelihood technique as in [19], where stationary behavior of the clutter and mine samples was assumed. Deming [21] proposed to use ML Adaptive Neural System (MLANS) to detect land mines. MLANS requires well defined clutter and mine signature models. The hand held system has nonstationary clutters and does not provide clear mine signatures. Hence MLANS would be more appropriate for the vehicle based system, and may not applicable to the hand held mine detection system. The above statistical techniques are operated in the full frequency band range domain data, and it is different from the proposed method where frequency domain data with subband processing is used.

Some preliminary results of the proposed detector were presented in part at conferences [22], [23]. This paper provides more detail descriptions and analysis of the proposed technique, and expands the experimental data sets to over 2300 mine targets of different types. For notation simplicity, we shall use bold face lower case letter to denote vector, bold face upper case letter to denote matrix, and normal face lower case letter to denote scalar.

The paper is organized as follows. The next section introduces the LP model for clutter samples, and examines the ML estimation of LP coefficients to be used in the computation of

test statistic. Section III discusses the adaptive threshold to account for the time-varying clutter behavior. Section IV describes the application of weighting matrices and examines the complexity of the proposed detector. Section V presents subband processing. Section VI examines the detection accuracy of the proposed method using over 2300 land mine targets and compares it to the differential energy detector. These targets consist mainly of buried anti-personnel land mines of different sizes, shapes and metal content (ranging from no metal to high metal content) that are collected from many sites under different soil conditions. Finally, the conclusion is drawn in Section VII.

II. Methodology

Let $\mathbf{x}(n) = [x_1(n), x_2(n), \ldots, x_L(n)]^T$ be a vector that contains the complex GPR return at position n. The element $x_i(n)$ is the radar return at frequency index i. The total number of frequency points available in each vector sample is L. As the radar head sweeps across the ground, a number of vector samples will be collected. The detection problem can be stated as follows: Given the current vector sample $\mathbf{x}(n)$ and a few previous vector samples, we wish to decide if $\mathbf{x}(n)$ is from a land mine. In other words, we are interested in performing the binary hypothesis test

$$H_0\text{: } \mathbf{x}(n) \text{ is from clutter,}$$
$$\text{versus}$$
$$H_1\text{: } \mathbf{x}(n) \text{ is from a land mine.}$$

Under H_0, the proposed method assumes that the current vector sample can be generated from a linear combination of its past few samples. That is, we assume that a clutter vector sample $\mathbf{x}(n)$ satisfies the time-varying LP model

$$\begin{aligned}\mathbf{x}(n) &= \sum_{k=1}^{P} a_k(n)\mathbf{x}(n-k) + \boldsymbol{\varepsilon}(n) \\ &= \mathbf{X}(n-1)\mathbf{a}(n) + \boldsymbol{\varepsilon}(n) \end{aligned} \tag{1}$$

where $a_k(n)$, $1 \le k \le P$ are the LP coefficients, P is the prediction order, $\boldsymbol{\varepsilon}(n)$ is the prediction error vector, the matrix $\mathbf{X}(n-1) = [\mathbf{x}(n-1), \mathbf{x}(n-2), \ldots, \mathbf{x}(n-P)]$ is the collection of P past GPR vector samples, and $\mathbf{a}(n) = [a_1(n), a_2(n), \ldots, a_P(n)]^T$ is the LP coefficient vector. Note that the linear prediction coefficients will be different at different position n. This is to take into account the human factors such as variations in sweeping speed and radar to ground distance, and the variations of clutter characteristics. The prediction coefficient vector $\mathbf{a}(n)$ and the prediction error vector $\boldsymbol{\varepsilon}(n)$ are complex because $\mathbf{x}(n)$ is complex. The model order P depends on the sweeping speed and larger order may be required for higher sweeping speed. In general, the radar signal is ultra-wide-bandwidth and propagated in a complexity of clutter sources under varying soil conditions. The distribution of the radar sample vector $\mathbf{x}(n)$ alone will not be Gaussian. However, after removing the time-varying components in $\mathbf{x}(n)$ through the LP model (1), the LP error vector $\boldsymbol{\varepsilon}(n)$ can reasonably be approximated to have Gaussian distribution with zero mean and covariance matrix $\mathbf{C}$. Hence the joint probability density function (pdf) of $\mathbf{x}(n)$ and $\mathbf{X}(n-1)$ under H_0 is

$$\begin{aligned} p(\mathbf{x}(n), \mathbf{X}(n-1); \mathbf{a}(n), H_0) \\ = \frac{1}{\pi^L \det(\mathbf{C})} \exp\{-(\mathbf{x}(n) - \mathbf{X}(n-1)\mathbf{a}(n))^* \\ \cdot \mathbf{C}^{-1}(\mathbf{x}(n) - \mathbf{X}(n-1)\mathbf{a}(n))\} \end{aligned} \tag{2}$$

where the superscript $*$ represents the complex conjugate transpose operation.

Under H_1, $\mathbf{x}(n)$ is very difficult to model. This is because land mine signatures are not consistent and only a small number of samples, say two, may contain the land mine return for small anti-personnel mines. Thus, the proposed method uses the CFAR strategy and is based on $p(\mathbf{x}(n), \mathbf{X}(n-1); \mathbf{a}(n), H_0)$ only. If Z_s is the space of $\mathbf{x}(n)$ for declaring a detection of mine, then the proposed technique selects Z_s to be the largest region such that the probability of false alarm is kept to a fixed level Γ, i.e.

$$\int_{Z_s} p(\mathbf{x}(n), \mathbf{X}(n-1); \mathbf{a}(n), H_0)\, d\mathbf{x}(n) = \Gamma. \tag{3}$$

Note that in our case Z_s is the region outside an ellipsoid to infinity. Since $p(\mathbf{x}(n), \mathbf{X}(n-1); \mathbf{a}(n), H_0)$ is Gaussian, the mine detection region corresponds to the range of $\mathbf{x}(n)$ such that

$$\begin{aligned} l(\mathbf{x}(n), \mathbf{X}(n-1); \mathbf{a}(n), H_0) = -(\mathbf{x}(n) - \mathbf{X}(n-1)\mathbf{a}(n))^* \\ \cdot \mathbf{C}^{-1}(\mathbf{x}(n) - \mathbf{X}(n-1)\mathbf{a}(n)) \end{aligned} \tag{4}$$

is less than or equal to some threshold. The proposed detector does not minimize the probability of error, which is a weighted sum of probability of miss and probability of false alarm according to the prior probabilities of mine and no mine. The proposed detector, however, is simple to implement and does not require the pdf of the measured data under H_1, which is difficult to model because of the inconsistent mine signatures in the hand held GPR system.

Denote the test statistic $\xi(n)$ as $-l(\mathbf{x}(n), \mathbf{X}(n-1); \mathbf{a}(n), H_0)$; $\xi(n)$ can be interpreted as the weighted prediction error. We declare a detection of mine if $\xi(n)$ is bigger than some threshold. The computation of the test statistic $\xi(n)$ requires the LP coefficient vector $\mathbf{a}(n)$, which is not known. We shall replace $\mathbf{a}(n)$ by its ML estimate for the computation of $\xi(n)$.

The ML estimate of $\mathbf{a}(n)$ is the value that maximizes the log likelihood (4). Taking the derivative of (4) with respect to $\mathbf{a}(n)$ and setting the gradient to zero gives the ML solution

$$\mathbf{a}^o(n) = (\mathbf{X}(n-1)^*\mathbf{C}^{-1}\mathbf{X}(n-1))^{-1}\mathbf{X}(n-1)^*\mathbf{C}^{-1}\mathbf{x}(n). \tag{5}$$

Substituting (5) into (4) simplifies the test statistic $\xi(n)$ to

$$\xi(n) = \mathbf{x}(n)^*\mathbf{C}^{-1}\mathbf{x}(n) - \mathbf{x}(n)^*\mathbf{C}^{-1}\mathbf{X}(n-1)\mathbf{a}^o(n). \tag{6}$$

A large test statistic value will indicate that the current vector sample $\mathbf{x}(n)$ is from a land mine. In practice, $\xi(n)$ is converted to the loudness of an alarm tone so that an operator of the hand

held detector can make a decision. For ease of illustration in this paper, we shall assume that H_1 will be selected if $\xi(n)$ is greater than some threshold TH.

III. Adaptive Threshold

Direct comparison of the test statistic $\xi(n)$ with a fixed threshold does not give satisfactory results. This is because the prediction error energy $\xi(n)$ may be time-varying, although the prediction coefficients $\mathbf{a}(n)$ have removed certain amounts of the nonstationarity in the clutter. Using a fixed threshold TH will increase the false alarm rate if the prediction error energy in the current clutter region is larger than expected, or decrease the probability of detection if the clutter prediction error energy is smaller than expected. The threshold TH should be made adaptive to improve performance. Experimental results indicate that making the threshold adaptive can reduce the false alarm rate (FAR) by as much as 40% at 90% probability of detection (Pd). It does not affect the results much for Pd below 80%. This section will first discuss the statistics for $\xi(n)$, and determine the relevant parameters that need to be updated on line in order to make the threshold adaptive.

The exact pdf of $\xi(n)$ in (6) is not easy to determine because it is a very complicated nonlinear function of $\mathbf{x}(n)$ and $\mathbf{X}(n-1)$. This is due to the fact that $\mathbf{a}^o(n)$ is an estimated value from the GPR vector samples. To simplify the study, we shall assume the estimation error in $\mathbf{a}(n)$ is small enough such that the estimation noise of $\mathbf{a}^o(n)$ can be neglected. Recall that $\boldsymbol{\epsilon}(n)$ is a zero mean Gaussian vector of covariance matrix $\mathbf{C}$. Under H_0, we have $\xi(n) = \boldsymbol{\epsilon}(n)^*\mathbf{C}^{-1}\boldsymbol{\epsilon}(n)$ so that $\xi(n)$ follows a chi-square pdf with L degrees of freedom [24]. GPR systems designed for land mine detection usually have a large number of frequency points L (for the experiments here, $L = 45$). When invoking the central limit theorem, the pdf of $\xi(n)$ can be approximated by a Gaussian whose distribution depends on mean and variance. The statistics of $\xi(n)$ change relatively slowly. Hence, the mean $\overline{\xi}(n)$ and variance $\sigma_\xi^2(n)$ are updated recursively through exponential averaging

$$\overline{\xi}(n) = (1-\lambda)\overline{\xi}(n-1) + \lambda\xi(n), \tag{7}$$

$$\sigma_\xi^2(n) = (1-\lambda)\sigma_\xi^2(n-1) + \lambda(\xi(n) - \overline{\xi}(n))^2 \tag{8}$$

where λ is the moving average parameter that has a positive small value. When variation of the clutter background is slow, a small value of λ should be used. From our experiments performed, a good range of λ is from 0.001 to 0.02.

Taking into account the time-varying mean and variance of the test statistic, we define the normalized test statistic as

$$\xi'(n) = \frac{\xi(n) - \overline{\xi}(n)}{\sigma_\xi(n)}. \tag{9}$$

$\xi'(n)$ can now compare against a fixed threshold TH' for detection. In effect, the threshold is multiplied by $\sigma_\xi(n)$ and translated by $\overline{\xi}(n)$ before it is compared against $\xi(n)$ for detection.

The purpose of (7) and (8) is to estimate the statistics of $\xi(n)$ in clutter. The update of the mean and variance of $\xi(n)$ should only take place if the current sample $\mathbf{x}(n)$ is from clutter and not from a land mine. Consequently, the update equations (7) and (8) should be applied at the present position n if the normalized test statistic $\xi'(n)$ is less than some value β. This is to ensure that the sample used for update is not likely to be from a land mine. Note that β and TH' are not necessarily the same.

Normally, β is set to a large value to maintain small amount of probability of false alarm so that most of the clutter samples are used to update the background statistics. In the current study, we found from experimentation that a good choice of β is between 3.0 and 3.5. Although a large β will have a higher chance of incorporating some mine samples to update the statistics, the corresponding effect on the estimation accuracy of clutter statistics will not be significant because the number of mine samples are small relative to the number of clutter samples and the exponential averaging in (7) and (8) will smooth out the effect of mine samples in the background clutter statistic update.

The choice of TH' is based on the tolerable false alarm rate for the hand held mine detection system. Note that it is not necessary to vary β when TH' changes.

IV. Weighting Matrix and Complexity

The test statistic $\xi(n)$ in (6) can be interpreted as the minimum weighted prediction error energy, where the weighting matrix $\mathbf{W}$ is given by $\mathbf{C}^{-1}$, the inverse of the covariance matrix of $\boldsymbol{\epsilon}(n)$ in clutter. The matrix $\mathbf{C}^{-1}$ can be decomposed into the product $\mathbf{C}^{-1/2}(\mathbf{C}^{-1/2})^*$. Defining $\tilde{\mathbf{x}}(n)$ as $(\mathbf{C}^{-1/2})^*\mathbf{x}(n)$, then (5) and (6) can be rewritten as

$$\mathbf{a}^o(n) = \left(\tilde{\mathbf{X}}(n-1)^*\tilde{\mathbf{X}}(n-1)\right)^{-1}\tilde{\mathbf{X}}(n-1)^*\tilde{\mathbf{x}}(n), \tag{10}$$

$$\xi(n) = \tilde{\mathbf{x}}(n)^*\tilde{\mathbf{x}}(n) - \tilde{\mathbf{x}}(n)^*\tilde{\mathbf{X}}(n-1)\mathbf{a}^o(n). \tag{11}$$

The number of frequency points L is large in practice so that the size of $\mathbf{C}$ is large. In addition, $\boldsymbol{\epsilon}(n)$ in clutter may be highly correlated. Hence the condition number of $\mathbf{C}$ can be very large and singularity problem may occur when taking the inverse of $\mathbf{C}$. To alleviate this problem, we reduce the rank of $\mathbf{C}$ before forming the weighting matrix. Let the eigen-decomposition of $\mathbf{C}$ be

$$\begin{aligned}\mathbf{C} &= \mathbf{Q}\boldsymbol{\Lambda}\mathbf{Q}^* \\ &= [\mathbf{q}_1, \mathbf{q}_2, \ldots, \mathbf{q}_L]\mathrm{diag}\{\lambda_1, \lambda_2, \ldots, \lambda_L\} \\ &\quad \cdot [\mathbf{q}_1, \mathbf{q}_2, \ldots, \mathbf{q}_L]^*\end{aligned} \tag{12}$$

where $\mathbf{Q}$ is the eigenvector matrix and $\boldsymbol{\Lambda}$ is the diagonal matrix of eigenvalues. Note that $\mathbf{Q}$ is complex and its eigenvector components $\mathbf{q}_i$, $i = 1, 2, \ldots, L$, are orthonormal. The eigenvalues are arranged in descending order, i.e., $\lambda_1 \geq \lambda_2 \geq \cdots \geq \lambda_L$. They are all real because $\mathbf{C}$ is complex conjugate symmetric. Let the tolerable condition number be K. We then form a $L \times L$ diagonal matrix $\mathbf{D}$ as

$$\mathbf{D} = \mathrm{diag}\{1/\lambda_1, 1/\lambda_2, \ldots, 1/\lambda_J, 0, 0, \ldots, 0\} \tag{13}$$

where J is the largest integer such that $(\lambda_1/\lambda_J) \leq K$. The weighting matrix is constructed as

$$\mathbf{W} = \mathbf{Q}\mathbf{D}\mathbf{Q}^*. \tag{14}$$

The corresponding transformed data vector is now equal to $\tilde{\mathbf{x}}(n) = \mathbf{D}^{1/2}\mathbf{Q}^*\mathbf{x}(n)$, where $\mathbf{D}^{1/2}$ is a diagonal matrix whose elements are the square-root of the elements in $\mathbf{D}$.

The clutter statistics are different at different geographical locations and soil types. In practice, the clutter covariance matrix $\mathbf{C}$ is estimated from a number of clutter samples collected in an area near the operation of the hand held detector. The weighting matrix is then computed from (14) and is fixed during the operation of the detector. The covariance matrix may need to be recomputed to provide accurate clutter characteristics after the detector has swept through a certain amount of area. Reducing the rank of $\mathbf{C}$ before forming $\mathbf{W}$ has an additional advantage that the weighting matrix contains only the principal components of the clutter characteristics that are relatively stable and does not have the minor components that will vary considerably during the operation of the detector unit.

Land mine detection requires real-time processing and it is beneficial to examine the computational complexity of the proposed method. One operation will represent one complex multiplication and one complex addition. We shall first look at the number of operations in computing $\mathbf{a}^o(n)$ from (10). The matrix $\tilde{\mathbf{X}}(n-1)$ has a shift structure, i.e., $\tilde{\mathbf{X}}(n-1)$ is $\tilde{\mathbf{X}}(n-2)$ by adding $\tilde{\mathbf{x}}(n-1)$ to the left and removing $\tilde{\mathbf{x}}(n-P-1)$ from the right. Hence the lower right $(L-1)\times(L-1)$ sub-matrix of $\tilde{\mathbf{X}}(n-1)^*\tilde{\mathbf{X}}(n-1)$ is equal to the upper left $(L-1)\times(L-1)$ sub-matrix of $\tilde{\mathbf{X}}(n-2)^*\tilde{\mathbf{X}}(n-2)$, and only the first row and first column of $\tilde{\mathbf{X}}(n-1)^*\tilde{\mathbf{X}}(n-1)$ need to be computed. Due to symmetry, the first row and column are identical. The elements in the first row, $\tilde{\mathbf{x}}^*(n-1)\tilde{\mathbf{x}}(n-1)$ and $\tilde{\mathbf{x}}^*(n-1)\tilde{\mathbf{x}}(n-j)$, $2 \le j \le P$ have already been computed in the previous instant $n-1$ when calculating $\xi(n-1)$ and $\mathbf{a}^o(n-1)$. Hence no additional computation is needed to form $\tilde{\mathbf{X}}(n-1)^*\tilde{\mathbf{X}}(n-1)$. The inverse of $\tilde{\mathbf{X}}(n-1)^*\tilde{\mathbf{X}}(n-1)$ requires P^3 operations. Computing $\tilde{\mathbf{X}}(n-1)^*\tilde{\mathbf{x}}(n)$ needs LP operations, and the matrix–vector multiplication to form $\mathbf{a}^o(n)$ requires P^2 operations. Finally, calculating $\xi(n)$ from (11) requires $L+P$ operations only since $\tilde{\mathbf{x}}(n)^*\tilde{\mathbf{X}}(n-1)$ has already been computed when calculating $\mathbf{a}^o(n)$. The total complexity in calculating the test statistic value is therefore

$$R = (P+1)L + P^3 + P^2 + P. \tag{15}$$

This expression is linear in the number of frequency samples and cubic in the number of previous samples (P) in the prediction model. In our experiences, L is typically between 40 and 128 whereas P is between 1 and 4. Therefore the computation is easily implemented in real-time. We now look at the complexity to generate $\tilde{\mathbf{x}}(n)$. Using $\mathbf{C}^{-1}$ as the weighting matrix takes L^2 operation. If the rank reduced weighting matrix is used instead, the number of operations is JL since only the first J eigenvectors of $\mathbf{C}$ are kept. In the special case when no weighting is used, $\tilde{\mathbf{x}}(n)$ is equal to $\mathbf{x}(n)$ and no additional computation is needed. Table I summarizes the computational complexity of the proposed method with different weighting matrices. The quantity R represents the number of operations shown in (15). In practice, the number of frequency points L is much larger than the prediction order P. The complexity will be dominated by the terms that contain L. The last row in Table I gives the order of operations of with and without weighting cases.

V. Subband Processing

The proposed LP based landmine detection method can be applied in either the time domain or the frequency domain. In fact, if the linear prediction detector (LPD) is applied to the time domain data, i.e., the inverse Discrete Fourier Transform of $\mathbf{x}(n)$, identical performance is expected because the Fourier transform is a unitary transform. One advantage of processing in the frequency domain is that the detection can be done in several frequency bands separately. This allows us to take into account the different land mine responses and clutter behaviors in different frequency regions. We shall generalize the proposed land mine detection method for subband processing.

Subband processing decomposes each frequency domain vector sample $\mathbf{x}(n)$ into M subvectors $\mathbf{x}_i(n)$, where $\mathbf{x}_i(n) = [x_{b_i}(n), x_{b_i+1}(n), \ldots, x_{e_i}(n)]^T$, $(b_i : e_i)$ is the frequency index range for band i, and $1 \le i \le M$. Note that the frequency bands can overlap so that b_{i+1} can be less than or equal to e_i. In some cases, windowing in the frequency bands may be desirable to minimize the band edge effect. The frequency bands $(b_i : e_i)$ are chosen to capture different landmine characteristics and clutter behaviors in different frequency regions. The number of frequency bands and the band edge frequencies are dependent on the frequency range that the GPR is operating. For the GPR used in this study, two bands are sufficient.

After band splitting, the LPD will be applied to the M frequency bands separately. The LPD produces the ML prediction coefficient vector $\mathbf{a}_i^o(n)$ and the test statistic $\xi_i(n)$. After normalization in each subband, M normalized test statistics $\xi_i'(n)$, $1 \le i \le M$, are available for detection.

There are many ways to combine the test statistics in the frequency bands for detection. From the collected data, the geometric mean of $\xi_i'(n)$ provides better performance than weighted sum in terms of lower false alarm rate at a given probability of detection. The geometric mean will be used here in the experimental study. The total test statistic to make the final decision is

$$\xi'(n) = \prod_{i=1}^{M} \{\xi_i'(n)\}^{1/p_i} \tag{16}$$

where $(1/p_1) + (1/p_2) + \cdots + (1/p_M) = 1$, $p_i \ge 1$, and $\xi_i'(n)$, $1 \le i \le M$ are assumed larger than one. The factors p_i are used to emphasize certain frequency bands where the land mine characteristics will appear, and/or to de-emphasize the frequency bands that are dominated by the clutter behavior. For frequency bands with significant land mine characteristics and relatively low clutter responses, the p_i should be set to smaller values. For instance, in the two subband case, if the lower band contains most of the mine characteristics, then p_1 should be smaller than p_2, such as $p_1 = 3/2$ and $p_1 = 3$. Good values of p_i can be found through optimizing (16). Since we would like $\xi'(n)$ to have large values for mine data and small values for clutter data, p_i can be chosen to maximize

TABLE I
COMPUTATIONAL COMPLEXITY OF THE PROPOSED METHOD

Weighting Matrix	$\mathbf{C}^{-1}$	$\mathbf{Q}\mathbf{D}\mathbf{Q}^T$	None
Complexity (Complex Operations)	L^2+R	$JL+R$	R
Complexity (Order of Operations)	$(L+P)L$	$(J+P)L$	PL

TABLE II
NUMBER OF DIFFERENT KINDS OF MINES IN THE DATA SETS

	Anti-Personnel	Anti-Tank
Low Metal Content	1032	923
High Metal Content	244	164

$\overline{\xi}'_{Mine} - \overline{\xi}'_{Clutter}$, where $\overline{\xi}'_{Mine}$ denotes the average detection value computed from mine training samples and $\overline{\xi}'_{Clutter}$ denotes the average detection value computed from clutter training samples. This is the method to choose p_i in this study.

VI. EXPERIMENTAL RESULTS

This section presents the detection results for the proposed LPD. The data for performance evaluation were collected at 5 different sites, under different weather conditions and soil types. The total number of land mine signatures is 2363. The land mines for detection are very diverse, ranging from small plastic anti-personnel mines to large metal anti-tank mines. Table II tabulates the number of mines in the data sets in terms of metal content and types. The data were collected at two different modes. The first is standing mode where the operator stands still and sweeps the hand held unit back and forth at a particular location to collect the data. The second is walking mode where the operator collects the data while walking. The data from each measurement site contains both operating modes. About 8% of the targets in each mine category shown in Table II are from walking mode. In addition to the mine data, clutter data were also measured when there were no mines under the ground. The number of clutter files is more than 800, and each clutter file has around 300 clutter vector samples. We shall first evaluate the detection accuracy of the proposed LPD, and compare it with the differential energy detector. Then the results for full band and subband processing will be contrasted. Finally, the effect of weighting matrix will be examined.

The LPD results were generated using (10) and (11) to compute the test statistic $\xi(n)$, and (9) for normalization before comparing to a threshold. The mean and variance for normalization were updated continuously using (7) and (8). The results are shown in the form of receiver operating characteristics (ROC) curves; the plots of the probability of detection (Pd) versus the false alarm rate (FAR). Pd is calculated by taking the ratio of the number of detected land mines to the total number of land mines. The FAR is computed over the clutter files only. It is not a probability of false alarm but it is related to the number of false alarms per unit time. This measure can be used as a relative measure to compare algorithms and evaluate the effectiveness of algorithm variations.

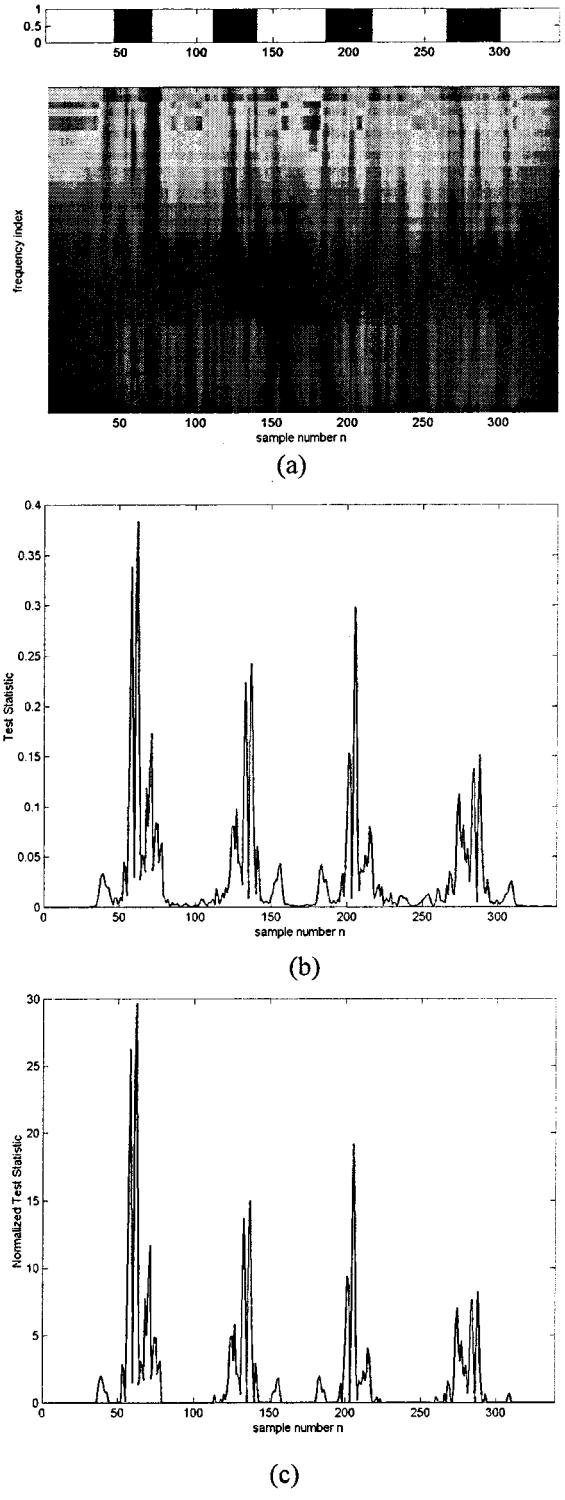

Fig. 3. (a) Land mine data image, (b) test statistic $\xi(n)$, and (c) normalized test statistic $\xi'(n)$.

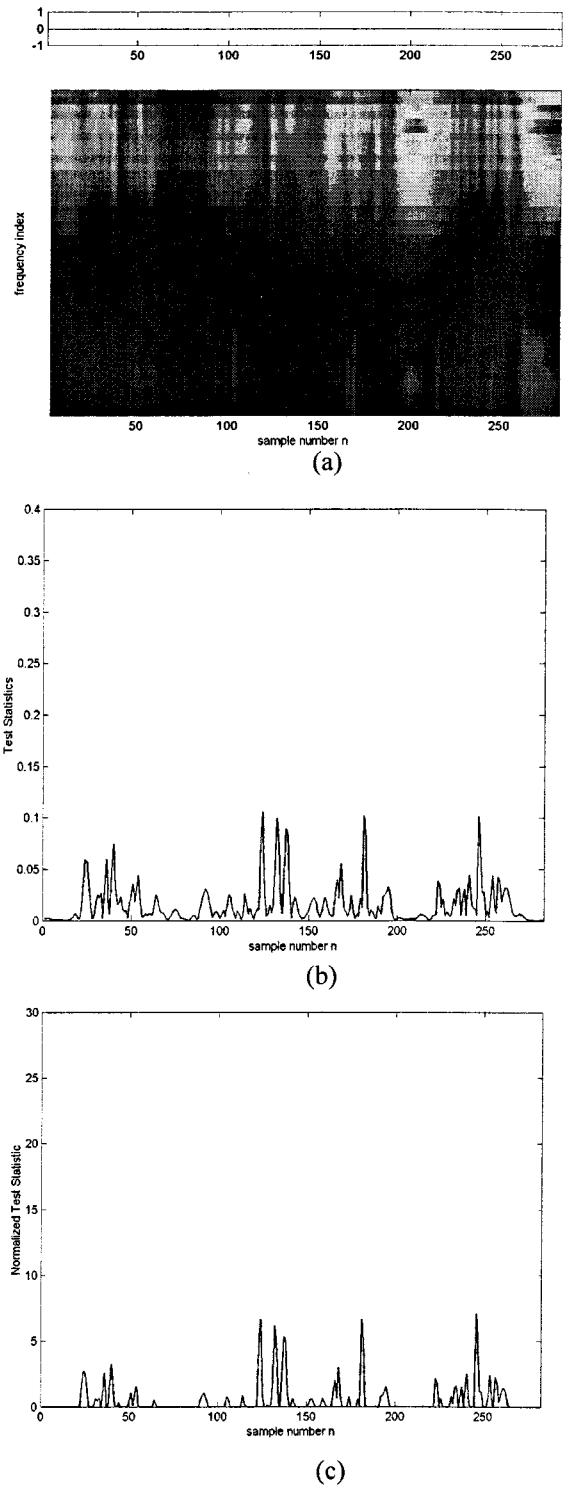

Fig. 4. (a) Land clutter data image, (b) test statistic $\xi(n)$, and (c) normalized test statistic $\xi'(n)$.

Each point in the ROC curve corresponds to a particular threshold setting. At each threshold, the number of detected mines is the number of mine data regions that have detection values bigger than the threshold. The FAR is the number of false alarms divided by the time duration in collecting data. The number of false alarms is equal to the ceiling of the number of clutter samples that exceed the threshold divided by the alarm size, where the alarm size is five samples. This alarm size corresponds to a target size of about 4 in. The duration in collecting data is set to the total number of samples divided by the data sampling rate. A large Pd corresponds to a small threshold value and a small Pd corresponds to a large threshold value.

A. Linear Prediction Land Mine Detection

We consider here a first order two-step LPD. That is, $P = 2$ and $a_1(n) = a_1 = 0$. The weighting matrix $\mathbf{W}$ was set to unity, that is $\tilde{\mathbf{X}}(n-1) = \mathbf{X}(n-1)$ and $\tilde{\mathbf{x}}(n-1) = \mathbf{x}(n-1)$. Fig. 3(b) depicts the LPD outputs $\xi(n)$ computed from (10) and (11) for a land mine file shown in Fig. 3(a). Although the land mine data plot in Fig. 3(a) does not provide visible indication of the presence of land mines the LPD is able to locate the land mine accurately and produces large $\xi(n)$ values for detection. Fig. 4(b) is the LPD outputs for a clutter file shown in Fig. 4(a) that was measured at the same lane as the land mine file. The LPD is able to account for the slow varying behavior of the clutter characteristics and produces relatively small values of $\xi(n)$ to reduce false detection. Figs. 3(c) and 4(c) are the normalized test statistics for the comparison against a fixed threshold for detection.

Fig. 5 gives ROC curves for the LPD. The normalization for adaptive threshold implementation used a moving average parameter λ of 0.01 in (7) and (8) and a β value of 3.5. They were chosen to yield the best results over the entire data sets available. This value of β corresponds to using 99.98% of the clutter samples [assuming Gaussian distribution of $\xi(n)$] to update the clutter background statistics. The value of λ was chosen based on how quickly the background clutter characteristics varied. In this experiment, both λ and β are fixed. They can be varied to obtain better performance if some knowledge about the soil condition and sweeping speed is available. The natural logarithm was applied to $\xi'(n)$ to reduce the dynamic range before scoring. Fig. 5(a) is for soil types gravel, dirt and sand. The number of land mine targets here is 1795. Fig. 5(b) is for soil types grass and offroad, and the number of targets is 568. The soil types have a significant effect in the land mine detection accuracy. For the first class of soil types, the detector achieves 90% Pd at a FAR of 0.7. For grass and offroad soil types, the FAR needs to be 1 to achieve the same Pd. The performance of the differential energy detector is also shown for comparison. This method applies energy detector [24] on the difference between the current sample and the most recent past sample for detection. We chose differential energy detector for comparison because it has comparable complexity with the proposed method and is near optimum in the statistical sense when the clutter characteristics are stationary and the Gaussian assumption holds. Normalization of detection value using (10) was used. The improvement of the prediction based method over the differential energy detector is significant. The reduction in FAR is 12% at 90% Pd for the first class of soil types, and is 28% for the second class of soil types. Fig. 5(c) is the combined ROC curves for all the soil types that contain 2363 targets. The proposed method reaches 90% Pd at a FAR of 0.8, while the differential energy detector requires a FAR of 1 to reach the same Pd.

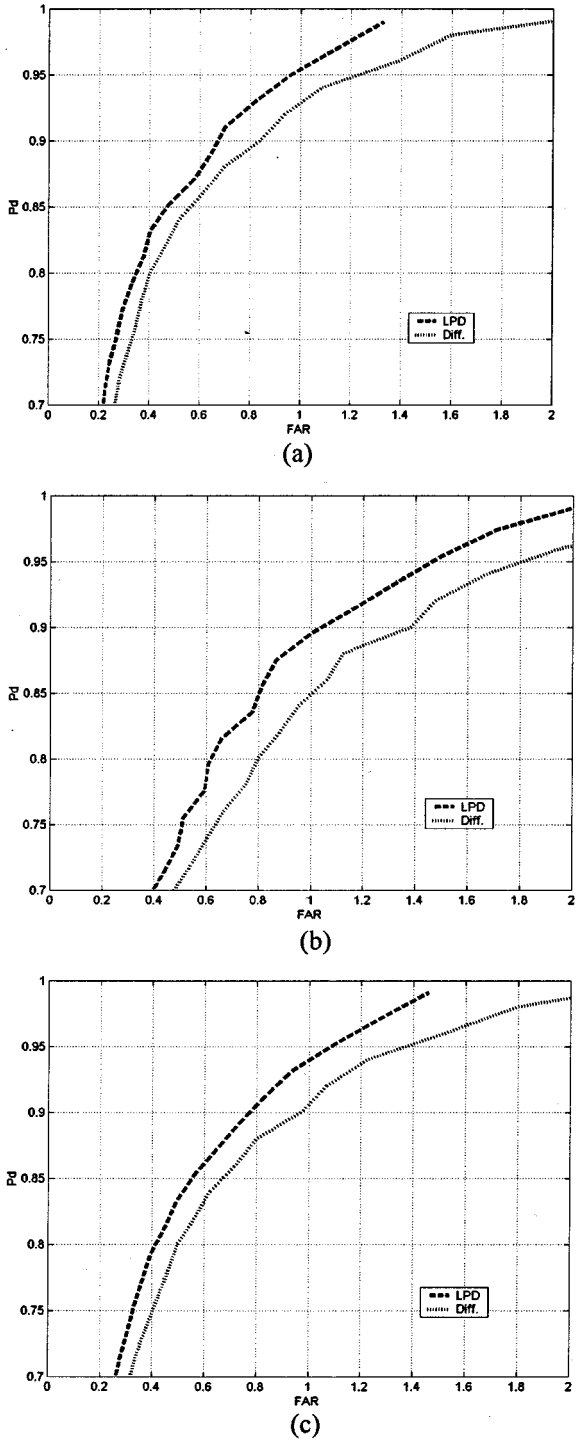

Fig. 5. ROC curve comparison between the proposed linear prediction detector (LPD) without subband processing and the differential energy detector (Diff): (a) soil types gravel, dirt, and sand, (b) soil types grass and offroad, and (c) all soil types.

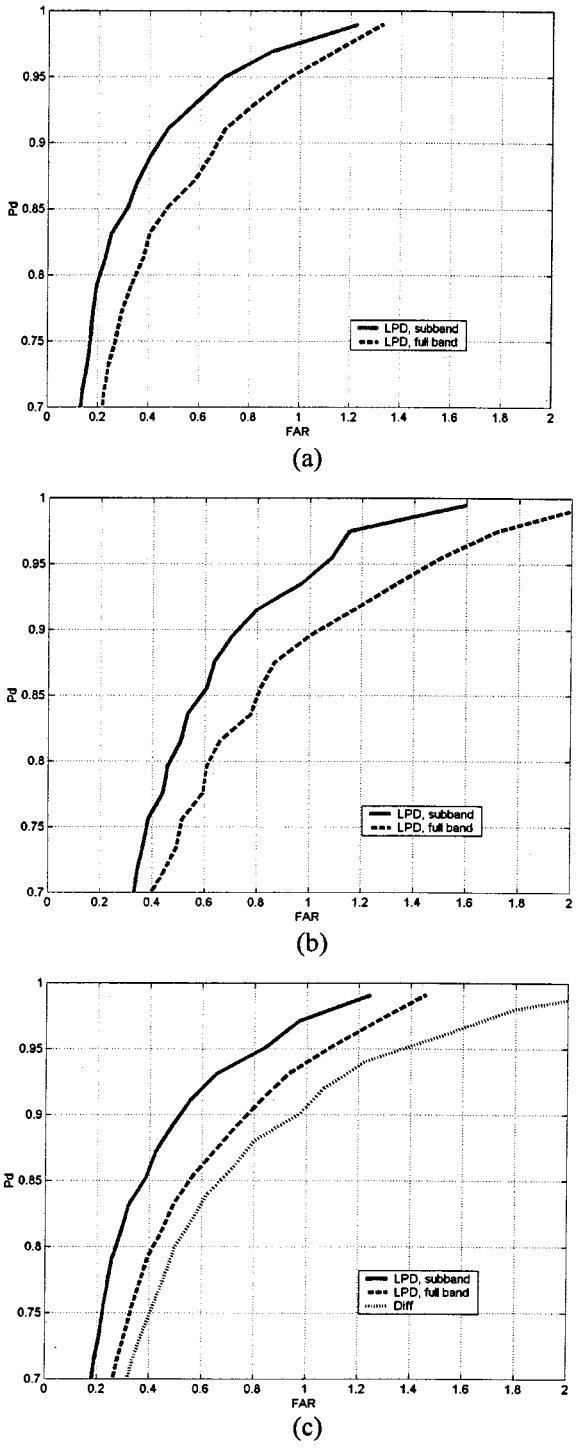

Fig. 6. ROC curve comparison of 2-subband LPD, full band LPD and differential energy detector (Diff): (a) soil types gravel, dirt and sand, (b) soil types grass and offroad, and (c) all soil types.

B. Subband Processing

In the previous subsection, the proposed method used the full frequency band to generate the results. This subsection investigates the performance of subband processing and compares the results with the full band case.

This simulation used two subbands: lower frequency band and upper frequency band. Hanning window is used in the separation of the two bands. Subband processing applies LPD separately in the two frequency bands to generate the normalized test statistics $\xi_1'(n)$ and $\xi_2'(n)$. Both frequency bands use a first order two-step predictor. To simplify computation, no weighting matrix is applied to the prediction errors when forming $\xi_i(n)$. The moving average parameter λ is 0.01 and β is 3.5 in the lower band. In the upper frequency band, λ is 0.000 01 and β is 3.5. A much smaller λ is used in the upper band because its detection

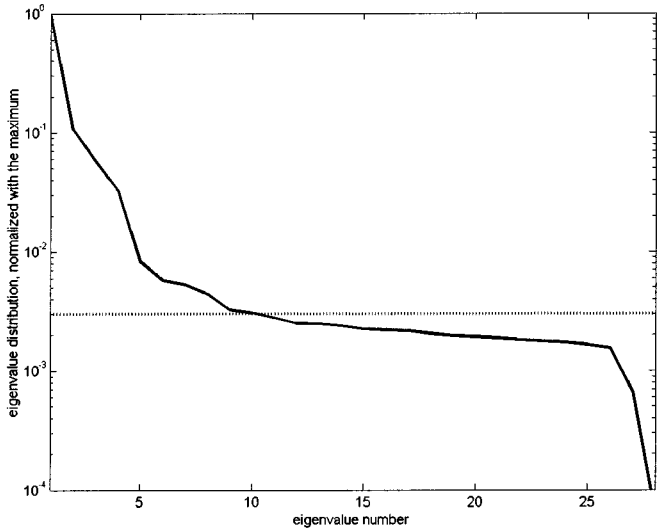

Fig. 7. Distribution of eigenvalues in the clutter covariance matrix $\mathbf{C}$. The eigenvalues are normalized with the maximum and the dotted line is at $1/K = 0.003$.

values are relatively stationary compared to the lower frequency band. The final test statistic for decision making is generated from (16), where p_1 and p_2 are found by optimization and are both set to 2. The natural logarithm is applied to the normalized test statistic $\xi'(n)$ to reduce its dynamic range before scoring.

Fig. 6 compares the ROC curves for full band and subband processing. Fig. 6(a) is for soil types gravel, dirt and sand, and Fig. 6(b) is for soil types grass and offroad. It is obvious from Fig. 6 that subband processing provides much better results than full band processing. In addition, the improvement is larger for soil types gravel, dirt and sand. For instance, at 90% Pd, subband processing reduces the FAR by 35% for soil types gravel, dirt and sand, and 28% for soil types grass and offroad. The overall ROC curves for all 2363 targets are depicted in Fig. 6(c). Subband processing has a FAR of 0.5 at 90% Pd, while full band processing has a much higher FAR of 0.8 at the same Pd. Finally, comparing Figs. 5(c) and 6(c) shows that the proposed LPD with two subbands gives 50% reduction of FAR at 90% Pd over the differential energy detector.

C. Effect of Weighting

The previous simulations did not apply the weighting matrix when computing the test statistic. This subsection examines the effect of weighting on the detection accuracy. For the weighting case, a first order two-step predictor was used in the LPD. The moving average parameter λ was 0.015 and the β value was 3.0 in the lower band. In the upper frequency band, λ was 0.000 03 and β was 3.0. Only the upper band applied weighting and the weighting matrix was set according to (14) with the condition number K set to 333. The covariance matrix $\mathbf{C}$ was generated from the training clutter data before detection. This value of K corresponds to the corner point in the distribution of the eigenvalues of $\mathbf{C}$, as is shown in Fig. 7. Fig. 8 compares the ROC curves for the 2-subband LPD with and without weighting under different soil conditions. In the case of without weighting, λ and β were set to the values in Section VI-B to give the best performance curve. Incorporating the weighting matrix improves

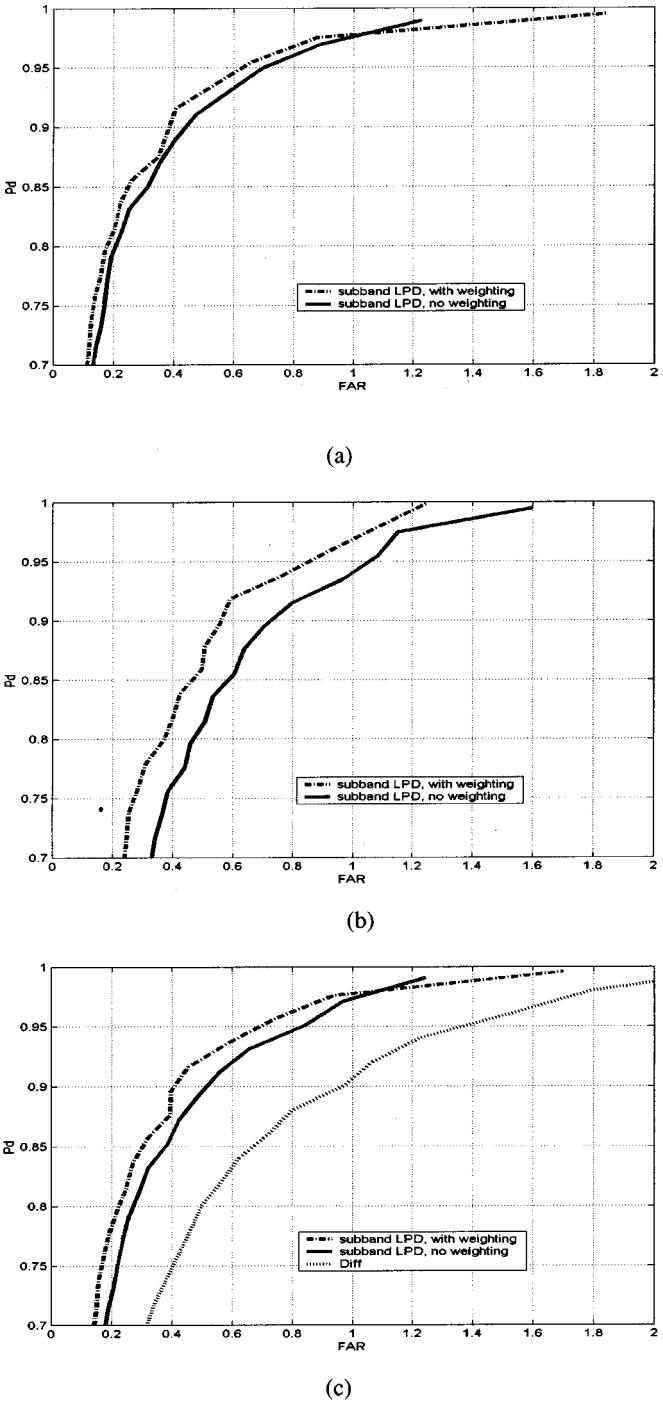

Fig. 8. ROC curve comparison of 2-subband LPD with weighting, 2-subband LPD without weighting and differential energy detector (Diff): (a) soil types gravel, dirt and sand, (b) soil types grass and offroad, and (c) all soil types.

the detection accuracy. The improvement is larger for soil types grass and offroad than for soil types gravel, dirt and sand. In total, the improvement is about 20% at 90% Pd over all the targets. Also shown in Fig. 8(c) is the ROC curve from differential energy detector. Comparing with the sample differencing detector, the weighted subband LPD reduces the FAR by 60% at 90% Pd.

Fig. 9 depicts the ROC curves for 55 difficult to find mine targets. The LPD with weighting outperforms the case without

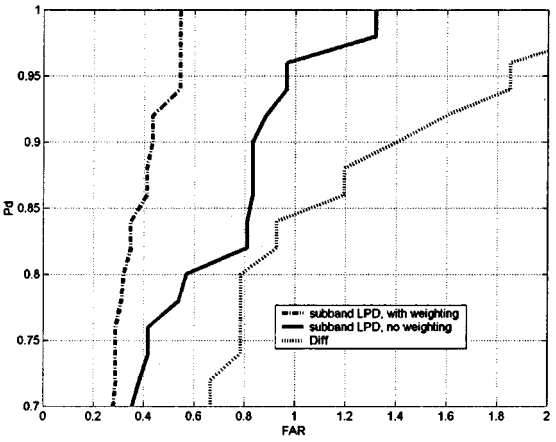

Fig. 9. ROC curve comparison of 2-subband LPD with weighting, 2-subband LPD without weighting and differential energy detector (Diff), 55 difficult to find mine targets.

TABLE III
FAR OF DIFFERENT DETECTION METHODS FOR STANDING TARGETS AND WALKING TARGETS

FAR, Standing Targets (2195)				
Pd	DF	FB-LPD	LPD	WLPD
90%	1	0.8	0.54	0.45
95%	1.4	1.15	0.82	0.72
FAR, Walking Targets (168)				
Pd	DF	FB-LPD	LPD	WLPD
90%	0.6	0.52	0.46	0.24
95%	0.88	0.84	0.78	0.44

DF: differential energy detector
FB-LPD: full band LPD
LPD: 2–subband LPD
WLPD: 2–subband LPD with weighting

weighting. The improvement is 50% decrease in FAR at 90% Pd. Applying weighting seems to be especially useful in detecting difficult to find land mines. Comparing with the differential energy detector, the reduction in FAR is 70% at 90% Pd.

The results shown in Figs. 5, 6, 8, and 9 are the aggregate performance for standing and walking targets. The following table lists separately the detection performance for the standing and walking targets. Among the total 2363 targets, 2195 targets are from standing mode and 168 targets are from walking mode. The walking target has a higher detection rate because only the largest confidence among four walking sweeps was used for detection. This is to take into account that only one walking sweep among the four had a land mine directly under the GPR. Table III indicates that in both standing and walking targets, the proposed LPD with weighting reduces the FAR by a factor of 2 compared to the baseline differential energy detector.

VII. CONCLUSIONS

This paper proposed a computationally efficient method that is based on the linear prediction for land mine detection. The GPR vector samples are varying slowly under clutter and are modeled by a linear prediction model. The proposed detector uses the CFAR technique and the likelihood function of clutter samples for detection. The computation of the test statistic requires the prediction coefficients, which are unknown and time-varying. ML technique is applied to determine the prediction coefficients, which are then used in the likelihood function to form the test statistic for detection. In order to account for the time-varying nature of the prediction error energy in background clutter, the mean and variance of the test statistic are updated recursively. The normalized test statistic with respect to mean and variance is compared against a fixed threshold for detection. Simulation results show that the proposed linear prediction detector outperforms the differential energy detector.

To further improve performance, we propose subband processing where each frequency domain data vector is split into several bands and LPD is applied to the subbands separately. The individual test statistics from different frequency bands are combined to form the final test statistic for decision making. Experimental results indicate that subband processing reduces FAR significantly and provides much better performance than full band processing.

Finally, the effect of weighting has been investigated in the proposed LPD. Experimental results indicate that incorporating weighting matrix improves the detector performance. The weighting matrix is especially useful in detecting difficult to find land mines. Overall, at 90% Pd, 60% reduction in FAR were obtained on all mines by the proposed method, and 70% reduction for difficult to find mines.

ACKNOWLEDGMENT

The authors would like to thank S. Burke, R. Weaver, R. Guckert, M. Locke, D. Sherbourne, L. Nee, P. Ngan, T. Broach, and J. Harvey for their support of this research, W. Steinway, H. Duvoisin, G. Solomon, and E. Bartosz for providing data and technical insights, and the reviewers for their comments and suggestions, which have been useful in improving the quality of the paper.

REFERENCES

[1] C. M. Rappaport and D. M. Reidy, "Focused array radar for real time imaging and detection," in *Proc. SPIE'96 Conf.*, Orlando, FL, 1996.
[2] M. D. Patz and M. A. Belkerdid, "Evaluation of a model-based inversion algorithm for GPR signal processing correlation for target classification," in *Proc. SPIE'98 Conf.*, Orlando, FL, 1998.
[3] T. R. Witten, "Present state of the art in ground-penetrating radars for mine detection," in *Proc. SPIE'98 Conf.*, Orlando, FL, 1998.
[4] P. D. Gader, H. Frigui, B. Nelson, G. Vaillette, and J. M. Keller, "New results in fuzzy set based detection of landmines with GPR," in *Proc. SPIE'99 Conf.*, Orlando, FL, 1999.
[5] P. D. Gader, B. Nelson, H. Frigui, G. Vaillette, and J. M. Keller, "Fuzzy logic detection of landmines with ground penetrating radar," *Signal Process., Spec. Issue Fuzzy Logic Signal Process. (Invited Paper)*, vol. 80, no. 6, pp. 1069–1084, June 2000.
[6] P. D. Gader, B. N. Nelson, A. Koksal Hocaoglu, S. Auephanwiriyakul, and M. A. Khabou, "Neural versus heuristic development of Choquet fuzzy integral fusion algorithms for land mine detection," in *Neuro-Fuzzy Pattern Recognition*, H. Bunke and A. Kandel, Eds, Singapore: World Scientific, 2000.
[7] P. D. Gader and M. Mystkowski, "Applications of Hidden Markov Models to detecting landmines with ground penetrating radar," in *Proc. SPIE'99 Conf.*, Orlando, FL, 1999.

[8] P. D. Gader, M. Mystkowski, and Y. Zhao, "Application of Hidden Markov Models to landmine detection using ground penetrating radar," *IEEE Trans. Geosci. Remote Sensing*, vol. 39, pp. 1231–1244, June 2001.
[9] K. C. Ho and P. D. Gader, "Fusion of statistical deviance and HMM GPR algorithms for the mine hunter/killer system," in *Proc. SPIE'01 Conf.*, Orlando, FL, 2001.
[10] P. D. Gader, M. Mystkowski, and Y. Zhao, "Adaptive Hidden Markov Models for extended landmine detection," in *Proc. SPIE'01 Conf.*, Orlando, FL, 2001.
[11] W. J. Steinway and H. Duvoisin, "Hand held mine detection system (HSTAMIDS)," in *Proc. UXO/Countermine Forum*, Los Angeles, CA, 2000.
[12] R. Guckert, M. Locke, and P. Ngan, "HSTAMIDS red team experiences/lessons learned," in *Proc. UXO/Countermine Forum*, Los Angeles, CA, 2000.
[13] H. Brunzell, "Detection of shallowly buried objects using impulse radar," *IEEE Trans. Geosci. Remote Sensing*, vol. 37, pp. 875–886, Feb. 1999.
[14] K. M. Kim, C. Lee, and D. H. Youn, "Adaptive processing technique for enhanced CFAR detecting performance in active sonar systems," *IEEE Trans. Aerosp. Electron. Syst.*, vol. 36, pp. 693–700, Apr. 2000.
[15] R. Srinivasan, "Simulation of CFAR detection algorithms for arbitrary clutter distributions," *Proc. Inst. Elect. Eng.*, vol. 147, pp. 31–40, Feb. 2000.
[16] E. Conte, A. De Maio, and C. Galdi, "Signal detection in compound-Gaussian noise: Neyman–Pearson and CFAR detectors," *IEEE Trans. Signal Processing*, vol. 48, pp. 419–428, Feb. 2000.
[17] A. Farina and A. Protopapa, "New results on linear prediction for clutter cancellation," *IEEE Trans. Aerosp. Electron. Syst.*, vol. 24, pp. 275–286, May 1998.
[18] C. Yuan, M. R. Azimi-Sadjadi, J. E. Wilbur, and G. J. Dobeck, "Underwater target detection using multichannel subband adaptive filtering and high-order correlation schemes," *IEEE J. Oceanic Eng.*, vol. 25, pp. 192–205, Jan. 2000.
[19] H. Brunzell, "Clutter reduction and object detection in surface penetrating radar," in *Proc. Radar'97 Conf.*, 1997, pp. 688–691.
[20] U. Uschkerat, "Mine detection using a maximum likelihood estimator and in-field GPR data," in *Proc. IEEE Int. Radar'00 Conf.*, 2000, pp. 294–298.
[21] R. W. Deming, "Automatic buried mine detection using the maximum likelihood adaptive neural system (MLANS)," in *Proc. 1998 IEEE ISIC/CIRA/ISAS Joint Conf.*, Gaithersburg, MD, Sept. 1998, pp. 428–433.
[22] K. C. Ho and P. D. Gader, "Correlation based landmine detection using GPR," in *Proc. SPIE'00 Conf.*, Orlando, FL, 2000.
[23] ——, "Improved correlation based algorithm for hand-held landmine detector," in *Proc. SPIE'01 Conf.*, Orlando, FL, 2001.
[24] S. Kay, *Fundamentals of Statistical Signal Processing*. Englewood Cliffs, NJ: Prentice-Hall, 1998, vol. II.

K. C. Ho (S'89–M'91–SM'00) received the B.Sc. degree (with first class honors) in electronics and the Ph.D. degree in electronic engineering from the Chinese University of Hong Kong, in 1988 and 1991, respectively.

He was a Research Associate in the Department of Electrical and Computer Engineering, Royal Military College of Canada, Kingston, ON, from 1991 to 1994. He joined Bell-Northern Research in 1995 as Member of Scientific Staff. He was a member of the Faculty in the Department of Electrical Engineering, University of Saskatchewan, Saskatoon, SK, Canada, from September 1996 to August 1997. Since September 1997, he has been with the University of Missouri, Columbia, where he is presently an Assistant Professor in the Electrical Engineering Department. He is also an Adjunct Associate Professor in the Royal Military College of Canada. His research interests include statistical signal processing, landmine detection, wireless communications, source localization, wavelet transform, and the development efficient adaptive signal processing algorithms for various applications including landmine detection, echo cancellation, time delay estimation, and system identification. He has been active in the development of the ITU standard recommendation G.168: Digital Network Echo Cancellers since 1995. He is the Editor of *ITU Standard Recommendation G.168*. He has received three patents from the United States in the area of telecommunications.

Dr. Ho received the Croucher Foundation Studentship from 1988 to 1991.

Paul D. Gader (M'87–SM'99) received the Ph.D. degree for research in image processing from the University of Florida, Gainesville, in 1986.

He was a Senior Research Scientist at Honeywell Systems and Research Center, an Assistant Professor of Mathematics at the University of Wisconsin, Oshkosh, and a Research Engineer and Manager at the Environmental Research Institute of Michigan (ERIM). He joined the University of Missouri, Columbia, in 1991 as an Assistant Professor of electrical and computer engineering, and later became an Associate Professor. Since 2001, he has been with the Computer Information and Science Engineering Department, University of Florida, Gainesville. He has worked on a wide variety of basic and applied research problems, including mathematical morphology in image processing, medical imaging, landmine and unexploded ordnance detection, handwriting recognition and document analysis systems, automatic target recognition and object recognition, fuzzy sets in computer vision, and applied mathematics. He is currently very active in landmine detection algorithm research.

Dr. Gader served as Chair of the SPIE Image Algebra and Morphological Image Processing Conference from 1990 to 1995. He is an Associate Editor of the *Journal of Mathematical Imaging* and the *Journal of Electronic Imaging*.